JOURNAL OF CHEMICAL & ENGINEERING DATA

ARTICLE

pubs.acs.org/jced

Iron-Impregnated Weakly Basic Resin for the Removal of 2-Naphthalenesulfonic Acid from Aqueous Solution

Dongmei Jia,[†] Yuejin Li,[†] Xili Shang,[†] and Changhai Li*[,‡]

[†]Department of Chemistry and Chemical Engineering, Binzhou University, Binzhou 256603, China

[‡]Research Center of Chemical Engineering and Technology, Binzhou University, Binzhou 256603, China

ABSTRACT: Commercial grade weakly basic resin D301 was impregnated with iron through a simple method using ferric chloride as the precursor for removing of 2-naphthalenesulfonic acid (2-NSA) from aqueous solution and sewage. The characteristics of the D301 before and after iron-impregnation were examined using scanning electron microscopy, X-ray diffraction, and Fourier transform infrared spectroscopy. The influences of pH, initial concentration of 2-NSA, contact time, temperature, and coexisting salts on the adsorptive removal of 2-NSA from aqueous solution by iron-impregnated resin D301 (Fe-D301) were studied by batch adsorption experiments. The adsorption of 2-NSA was found strongly affected by the pH, with pH 2.8 providing maximum adsorption of 2-NSA from aqueous solutions. Langmuir, Freundlich, Redlich−Peterson, and Temkin isotherm models were applied to the experimental data. Thermodynamic parameters such as free energy, enthalpy, and entropy were calculated using van't Hoff equations, which showed that 2-NSA adsorption on Fe-D301 was spontaneous and exothermic. Column studies were conducted to examine the use of the adsorbent for the removal of 2-NSA from continuously flowing aqueous solutions. Fe-D301 synthesized in this study exhibited a higher affinity for 2-NSA and salt coexisting solution compared with references in literature and shows great potential in further field processes.

1. INTRODUCTION

Effluent-containing dye is one of the most difficult types of wastewater to treat, because of the presence of large quantities of poorly biodegradable and often toxic substances such as additives, detergents, surfactants, and textile auxiliary chemicals. One of these substances is 2-naphthalenesulfonic acid (2-NSA), which is an important dye intermediate and used as a textile auxiliary chemical.[1] 2-NSA contains one sulfonic group ($-HSO_3$). Effluent from dye manufacturing that contains 2-NSA can cause serious pollution and affect water quality when it is discharged into the environment.

Various techniques have been developed for the removal of dyes from water and wastewater. These include biological treatment,[2] coagulation,[3] ozone treatment,[4] chemical oxidation,[5,6] membrane filtration,[7] ion exchange,[8] photocatalytic degradation,[9,10] and adsorption.[11−14] Adsorption is a good technique for the removal of trace amounts of solutes from aqueous solution, because of its low cost, simple design, easy operation, potential for adsorbent recycling, and environmental friendliness.[15] Many adsorbents have been investigated for wastewater treatment, including activated carbon, sludge ash, cashew nut shells, and polymers.[16,17] Ion exchange resin is used to remove contaminants in water treatment processes because of its huge specific surface area and well-developed pore structures. In our previous study,[18] we used D301 resin for the adsorptive removal of 2-NSA from aqueous solution and found that a dramatic decrease in adsorption capacity was observed for D301 upon addition of Na_2SO_4 into the 2-naphthalenesulfonic acid solution. A review of literature shows that the adsorption capacity of adsorbent was increased significantly by surface modification.[19−21] Surface modification involves the functionalization of the adsorbent surface with new groups that may provide new sites for the adsorption of solutes from aqueous solutions. Many studies have focused on arsenic adsorption by iron-modified activated carbon and iron-impregnated ion exchange beads.[22−28] However, few reports have detailed use of the iron-impregnated resin to remove dyes and dye intermediates from wastewater.

In this article, a simple method was to use ferric salt solution as the precursor and precipitate ferric onto commercial weakly basic resin (D301). The iron-impregnated D301 (Fe-D301) structures were characterized using various analytical techniques. Fe-D301 was used as an adsorbent for the removal of 2-NSA from aqueous solutions. The influence of experimental parameters such as pH, contact time, initial 2-NSA concentration, temperature, and the presence of salts were studied. Column adsorption was used to evaluate the adsorption process for the removal of 2-NSA from aqueous solutions and sewage.

2. EXPERIMENTAL SECTION

2.1. Materials. 2-NSA (98.0% purity) was purchased from Sigma-Aldrich (St. Louis, MO). All other chemicals were of analytical grade and obtained from Shanghai Chemical Reagent Station (Shanghai, China). D301 resin was from Nankai Resin Co. Ltd. (Tianjin, China).

2.2. Adsorbent Preparation. Fe-D301 resin was prepared by soaking dry D301 resin in $FeCl_3$−HCl−NaCl solution (0.4 mol·dm^{-3} $FeCl_3$, 2.0 mol·dm^{-3} NaCl, and 0.2 mol·dm^{-3} HCl) for 72 h at 298 K. The mixture was then filtered and

Received: June 17, 2011
Accepted: August 17, 2011
Published: August 30, 2011

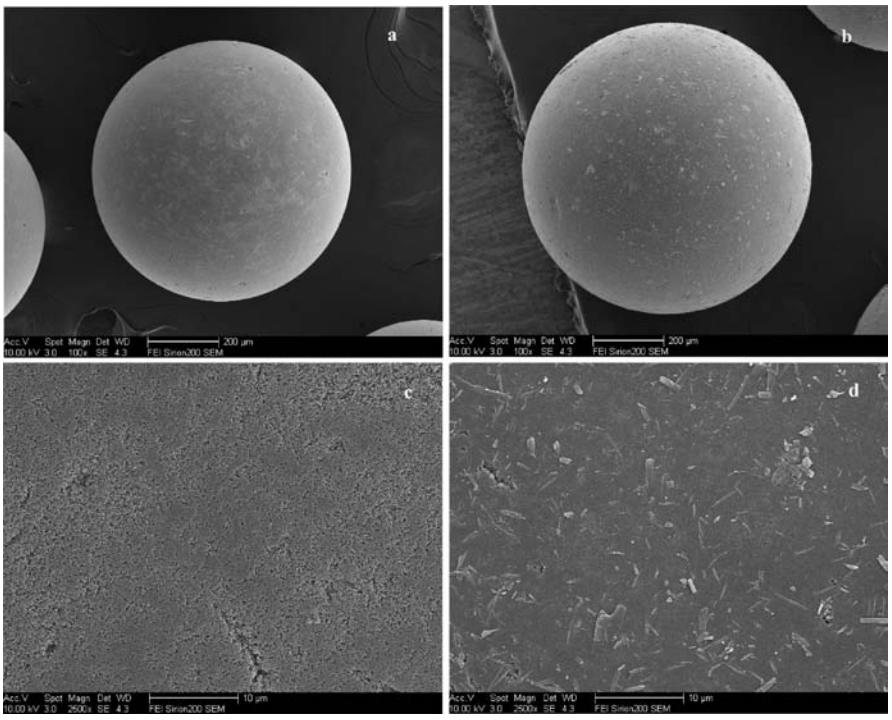

Figure 1. Morphology of resin (a, c) = D301 and (b, d) = Fe−D301.

rapidly added dropwise to a NaOH−NaCl solution (2.5 mol·dm^{-3} NaOH and 1.0 mol·dm^{-3} NaCl) to form Fe-D301. The Fe-D301 resin was filtered and washed with ethanol until no brown floc appeared and then washed with distilled water until the pH was neutral. Finally, it was dried at 313 K for 24 h and stored in an airtight container.

2.3. Adsorbent Characterization and Analytical Methods. Morphological analysis of the Fe-D301 resin was performed using field emission scanning electron microscopy (SEM, Sirion 200 FEI, Hillsboro, OR). Iron species were identified by X-ray diffraction (XRD, D/MAX-2500/PC, Rigaku, Tokyo, Japan). Fourier transform infrared (FT-IR) spectra for the D301 resins before and after their impregnation with iron were obtained using a NICOLET-380 FT-IR (Thermo Fischer Scientific, Waltham, MA). The Brunauer−Emmett−Teller (BET) surface area of the Fe-D301 resin was measured using an automated gas sorption system (3H-2000PS2, Bei Shide Instrument S&T Co. Ltd., Beijing, China).

2-NSA in solution was analyzed on a high-performance liquid chromatograph (LC-10AT, Shimadzu Corp., Kyoto, Japan) and a UV−vis spectrophotometer (10A VP, Shimadzu Corp., Kyoto, Japan). Separation was performed on a C18 analytical column (150 × 4.6 mm i.d., particle size 5 μm). The mobile phase was methanol−water (50:50, v/v) containing 0.5 % KH_2PO_4 as a pH regulator. The mobile phase flow rate was 0.8 cm^3·min^{-1}, and the detector wavelength was 275 nm. Sample solutions were filtered through 0.45 μm membrane filters, and the filtrates were analyzed for residual 2-NSA.[18]

2.4. Adsorption Studies. Batch adsorption studies were performed by mixing 0.100 g of resin particles with 100 cm^3 of 2-NSA solution at various concentrations [(100 to 1000) mg·dm^{-3}] in a 250 cm^3 glass flask at pH 2.8. To investigate the effect of pH, 100 cm^3 of 500 mg·dm^{-3} 2-NSA solution (pH 2.8 to 12.0) was mixed with 0.100 g of resin particles for 24 h to reach equilibrium. Sulfuric acid and sodium hydroxide were used to adjust the solution pH throughout the experiment when necessary. The effect of temperature [(298, 313, and 323) K] was investigated at pH 2.8 with 0.100 g of resin particles at various 2-NSA concentrations. Adsorption kinetic studies were conducted at pH 2.8 using 0.100 g of resin particles. The resin was added to 100 cm^3 of 500 mg·dm^{-3} 2-NSA, and the contact times ranged from (0.5 to 9) h. Samples were removed for 2-NSA concentration measurements at 30 min intervals.

The 2-NSA uptake capacity, q_e, at equilibrium (or at time, t) of the sorbent was calculated from the following mass balance relationship:[29]

$$q_e \quad (\text{or}) \quad q_t = \frac{(C_0 - C_e)V}{W} \tag{1}$$

where C_0, C_t, and C_e are the initial, at time t, and residual concentration (mg·dm^{-3}) of 2-NSA in solution, respectively; and V and W are the test solution volume (dm^3) and mass (g) of sorbent used for the test, respectively.

Column experiments were carried out with a glass column (ø 12 mm, length 230 mm) equipped with a water bath to maintain a constant temperature. A BT-200F pump was used to ensure a constant flow rate. All column runs were performed under hydrodynamic conditions at 298 K, with 1000 mg·dm^{-3} 2-NSA, a dry resin bed volume (BV) of 10 cm^3, and a liquid velocity of 3 BV·h^{-1}. During our experiments, three parallel measurements were performed at the same conditions, and an average value is given. The maximum standard deviation of each triplicate data is 0.19 %, and the minimum is 0.11 %.

3. RESULTS AND DISCUSSION

3.1. Adsorbent Characterization. SEM micrographs of the D301 resin are shown in Figure 1a,c, and those of the Fe-D301

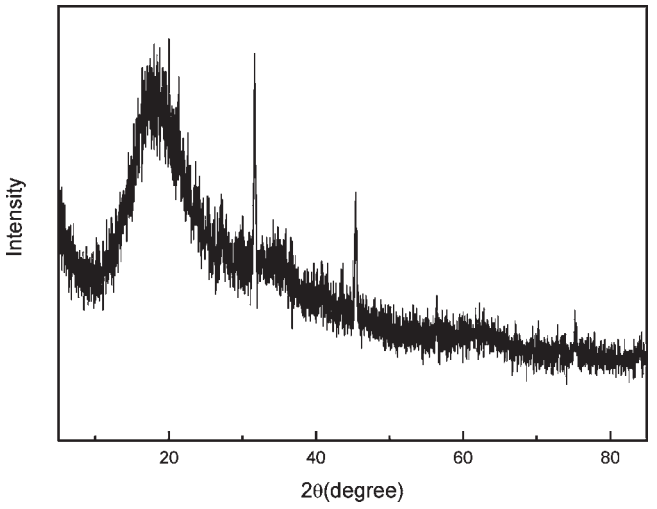

Figure 2. XRD spectra of Fe-D301.

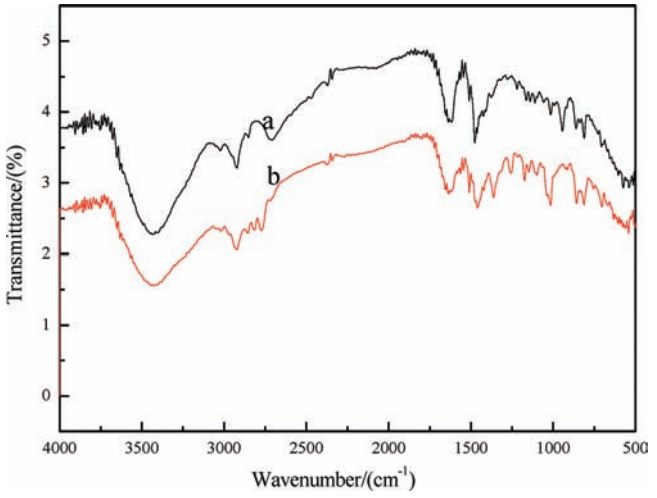

Figure 3. FTIR spectrum of resin. (a) D301; (b) Fe-D301.

resin are shown in Figure 1b,d. The iron was evenly distributed on the D301 resin (Figure 1d), and the surface morphology of Fe-D301 resin was different from that of the D301 resin. A rough surface and abundant pores would provide convenient diffusion channels for ions onto the Fe-D301 resins when they were used for adsorption in aqueous solution. The iron formed rod-shape particles (Figure 1d) approximately (1 to 4) μm in length and (0.1 to 0.5) μm in diameter in the macropores of D301. Some areas without iron rods were observed (Figure 1d). The presence of these areas suggests some parts of the resin contains micro- and mesopores, which are smaller in size than macropores and not large enough to allow the formation of rod-shape particles from the impregnated iron.

The XRD spectrum of Fe-D301 (Figure 2) showed that the impregnated iron in Fe-D301 was amorphous.

The FT-IR spectra of D301 and Fe-D301 are shown in Figure 3. The FT-IR spectrum of D301 shows a broad absorption band around 3300 cm^{-1}, which may be attributed to the O−H group. The bands at (2996 and 2869) cm^{-1} correspond to C−H stretching from the methylene group. The bands at (1637 and 1459) cm^{-1} are from aromatic C−C stretching in the phenyl

Table 1. Physical Characteristics of D301 and Fe-D301

	BET specific surface area	total pore volume	pore size
adsorbent	$m^2 \cdot g^{-1}$	$cm^3 \cdot g^{-1}$	nm
D301	29.06	0.13	17.51
Fe-D301	28.80	0.15	20.46

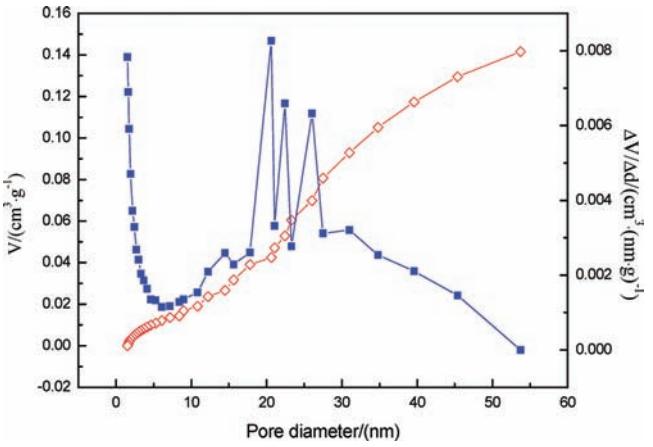

Figure 4. Microspore size distribution of Fe-D301. ◇, V; ■, $\Delta V/\Delta d$.

ring of lignin.[18] The band at 1477 cm^{-1} was associated with the C−H bending vibration of quaternary ammonium groups in the modified resin. The intense band at 1376 cm^{-1} corresponded to the characteristic C−N stretching vibration of amine groups in the resin.[30] The spectra indicated that the carbonyl group band was less intense and had shifted for of Fe-D301 compared to D301. There were also fewer bands in the fingerprint region of Fe-D301 compared to that of D301. The bands near 1625 cm^{-1} (Figure 3b) are from C−O functional groups in the fingerprint region of Fe-D301. It may be caused by a chemical bond between the impregnated iron and the resin. The bands at (424 and 408) cm^{-1} can be assigned to the stretching vibration of Fe−O in Fe-D301. Gong et al.[31] stated that the bands between (700 and 400) cm^{-1} are from Fe−O stretching vibration. The FT-IR spectrum of Fe-D301 has a weak band at 1037 cm^{-1} for Fe−OH.[32] These observations clearly indicate that iron impregnation of D301 occurred.

The BET surface area of Fe-D301 was 28.80 $m^2 \cdot g^{-1}$. Table 1 lists the physical characteristics of Fe-D301. After iron impregnation, the D301 resin surface area decreased slightly because of blockage of its pores by iron. However, the pore volume of the modified resin slightly increased. The pores of Fe-D301 resins were found to range in size from (1.7 to 46.6) nm (Figure 4). The micropore volume of the resin is increased slightly after modification.

3.2. Impact of pH on 2-NSA Adsorption. The pH is one of the most important factors affecting the adsorption process. Because 2-NSA and the surface charge of Fe-D301 in the liquid phase depend on pH, experiments were performed to find the optimum pH for adsorption of 2-NSA ions onto the Fe-D301 adsorbents. Different initial pH values ranging from 2.8 to 12.0 were investigated (Figure 5). The removal of 2-NSA was clearly pH-dependent, with the highest adsorption occurring at pH 2.8. In the lower pH region, positively charged sites dominate, and

dx.doi.org/10.1021/je2005984 |J. Chem. Eng. Data 2011, 56, 3881–3889

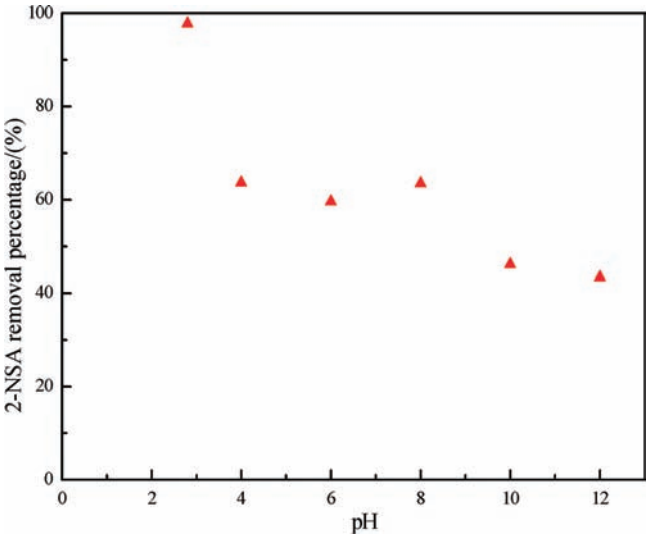

Figure 5. Effect of pH on the 2-NSA adsorption on Fe-D301 (initial 2-NSA concentration, 500 mg·dm^{-3}; contact time, 24 h; temperature, 298 K; agitation speed, 180 rpm).

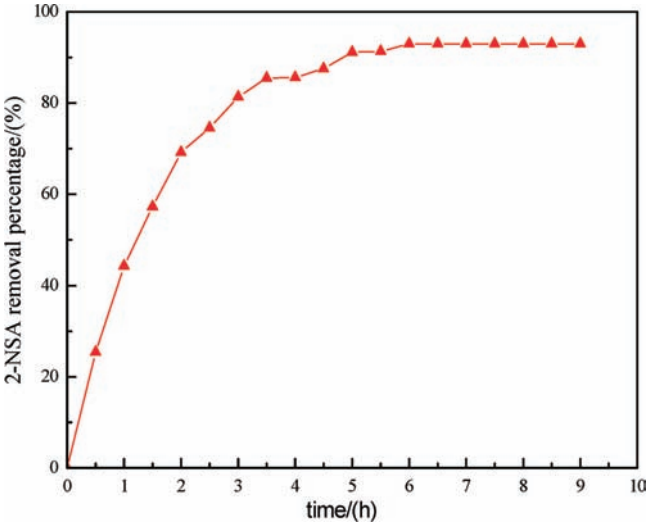

Figure 6. Effect of time for the adsorption of 2-NSA onto Fe-D301 (initial 2-NSA concentration, 500 mg·dm^{-3}; temperature, 298 K; agitation speed, 180 rpm).

this enhances the attractive forces between the sorbent surface and the 2-NSA ions, which subsequently increases the adsorption of 2-NSA ions. By contrast, at higher pH the deprotonation of sorbent surface is favored,[33,34] which increases the number of the negatively charged sites. This enhances repulsion between the sorbent surface and the 2-NSA and consequently decreases the adsorption capacity.

3.3. Effect of Contact Time and Initial Concentration. The adsorption of 2-NSA onto Fe-D301 was monitored for 9 h at 298 K. The initial 2-NSA concentration was 500 mg·dm^{-3}, and the initial pH was 2.8. 2-NSA was adsorbed onto Fe-D301 rapidly, and equilibrium was achieved within 6 h (Figure 6). The large specific surface area of the Fe-D301 resin could contribute to this result, because it favors diffusion of 2-NSA from the bulk solution onto the active sites of the adsorbent surface. External adsorption

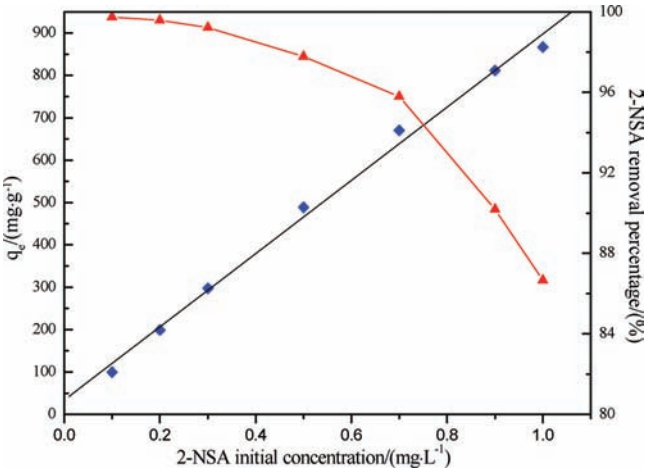

Figure 7. Effect of initial concentration for the adsorption of 2-NSA onto Fe-D301 (contact time, 24 h; temperature, 298 K; agitation speed, 180 rpm). ◆, q_e; ▲, removal percentage.

apparently dominated, and pore diffusion was observed to decrease the adsorption rate. A 24 h contact time was adopted for the subsequent experiment to ensure adsorption equilibrium was attained. The short equilibrium time is in agreement with other reports for the adsorption of other aromatic compounds onto resins.[18] In conventional porous adsorbents, adsorption occurs through pore diffusion, which decreases the adsorption rate. The iron-impregnated particles are nonporous adsorbents, and only external adsorption occurs. This type of adsorption mass transfer requires less time to reach equilibrium.[35] This result is promising as equilibrium time is important in determining the economic viability of a wastewater treatment plant.

More 2-NSA was adsorbed as the initial concentration of 2-NSA in solution also increased (Figure 7). This can be attributed to an increase in the ion occupancy number, which favors the adsorption process. The initial concentration of 2-NSA provided the necessary driving force to overcome mass-transfer resistance of 2-NSA between the aqueous and the solid phases. Hence, a higher initial metal concentration will be beneficial for the resin adsorption capacity. The equilibrium adsorption capacity appeared to increase linearly ($R^2 = 0.995$) as the initial metal concentration was increased from (100 to 1000) mg·dm^{-3}.

3.4. Effect of Temperature on 2-NSA Adsorption. The quantity of 2-NSA adsorbed onto Fe-D301 was investigated at different temperatures. Figure 8 shows temperature does not have a pronounced effect on the adsorption capacity of the adsorbents. It is found that the adsorption of 2-NSA decreases with an increase in temperature slightly. Since adsorption is an exothermic process, it would be expected that a decrease in temperature would result in an increase in the adsorption capacity of the adsorbent. The decrease in 2-NSA adsorption with temperature may be attributed to a decrease in solution viscosity and solubility, which in turn decreases the number of ions that interact with active sites at the adsorbent surface. This decrease suggests that the adsorption process is exothermic.[36] In this work, a study of temperature-dependent adsorption processes provides valuable information about the standard Gibbs free energy, enthalpy, and entropy changes accompanying adsorption.

3.5. Adsorption Isotherms. For a solid−liquid system, the adsorption isotherm is important for describing adsorption

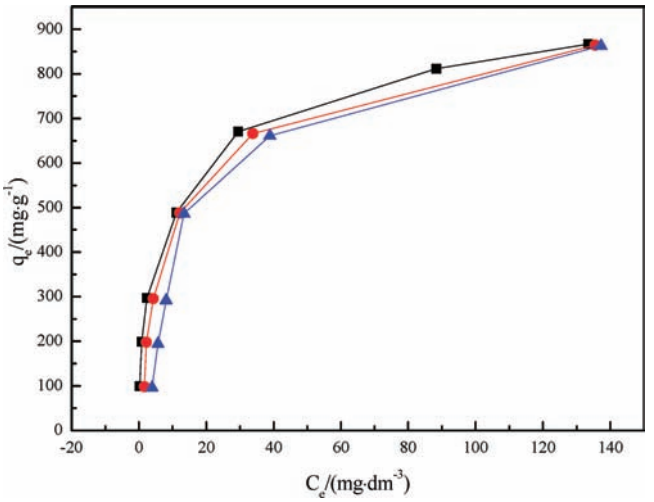

Figure 8. Effect of temperature on the adsorption of 2-NSA (initial 2-NSA concentration, (100 to 1000) mg·dm^{-3}; contact time, 24 h; agitation speed, 180 rpm). ■, 298 K; ●, 313 K; ▲, 323 K.

Table 2. Parameters for 2-NSA Adsorption by Fe-D301 According to Different Isotherm Models

isotherm	parameter	298 K	313 K	323 K
Langmuir	q_{max} (mg·g^{-1})	843.95	904.21	993.50
	b (dm^3·mg^{-1})	0.19	0.10	0.05
	R^2	0.947	0.988	0.964
Freundlich	k (mg·g^{-1})	236.79	181.43	133.16
	n	3.64	3.03	2.55
	R^2	0.973	0.911	0.857
Temkin	K_T (dm^3·mg^{-1})	6.01	1.29	0.48
	B_1 (kJ·mol^{-1})	126.94	171.41	216.30
	R^2	0.987	0.994	0.966
Redlich−Peterson	K_R (dm^3·g^{-1})	523.88	109.12	45.44
	b_R ((dm^3·mg^{-1})^m)	1.48	0.17	0.03
	m	0.81	0.92	1.11
	R^2	0.996	0.991	0.957

behavior. Adsorption isotherms are a constant−temperature equilibrium relationship between the amount of adsorbate per unit of adsorbent (q_e) and its equilibrium solution concentration (C_e). A number of mathematical models have been employed for describing this equilibrium relationship. In this work, the Langmuir, Freundlich, Redlich−Peterson, and Temkin isotherm models were used. Identifying the model that is the best fit for the data is critical for optimizing the adsorption process design.[37] The isotherm models were compared using the correlation coefficient, R^2, values.

3.5.1. Langmuir Isotherm. The Langmuir model generally expressed as follows:[38]

$$q_e = \frac{q_{max} b C_e}{1 + b C_e} \quad (2)$$

where q_e (mg·g^{-1}) and C_e (mg·dm^{-3}) are defined as the mass of 2-NSA adsorbed per unit weight of adsorbent and equilibrium liquid phase concentration, respectively; and q_{max} (mg·g^{-1}) is a constant related to the area occupied by a monolayer of adsorbate, which reflects the maximum adsorption capacity.

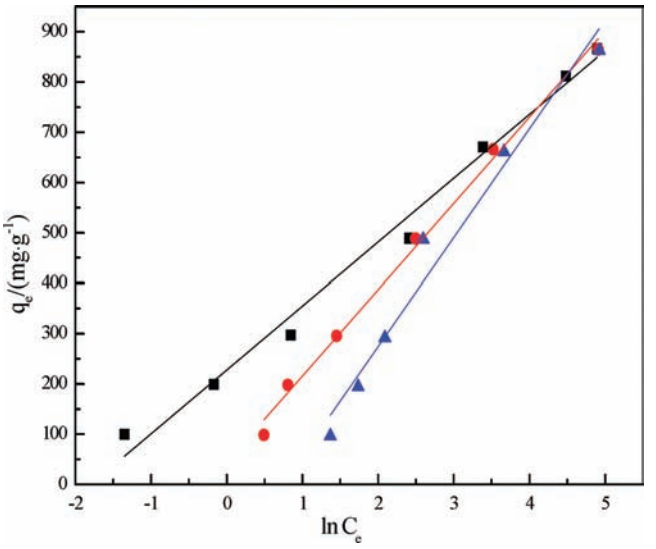

Figure 9. Temkin isotherm for adsorption of 2-NSA onto Fe-D301 (initial 2-NSA concentration, (100 to 1000) mg·dm^{-3}; contact time, 24 h; agitation speed, 180 rpm). ■, 298 K; ●, 313 K; ▲, 323 K; black line, line fit of 298 K; red line, line fit of 313 K; blue line, line fit of 323 K.

The q_{max} results from the Langmuir isotherm at (298, 313, and 323) K were (1843.95, 904.21, and 993.50) mg·g^{-1}, respectively, for 2-NSA (Table 2). The Fe-D301 had a high capacity for 2-NSA removal, which could be used in low-cost and readily available wastewater treatment.

3.5.2. Freundlich Isotherm. The Freundlich isotherm is an empirical equation employed to describe heterogeneous systems. The linear form of the Freundlich equation is as follows:[39]

$$q_e = k C_e^{1/n} \quad (3)$$

where k (mg·g^{-1}) and n are Freundlich constants. The constant k is defined as an adsorption or distribution coefficient and represents the mass of adsorbate adsorbed on an adsorbent for a unit equilibrium concentration. The model parameters calculated from linear plots and correlation coefficients are shown in Table 2. The n values ranged from 2 to 3 at different temperatures, which indicates adsorption was favorable.

3.5.3. Redlich−Peterson Isotherm. The Redlich−Peterson isotherm contains three parameters and incorporates the features of the Langmuir and the Freundlich isotherms.[40] The Redlich−Peterson isotherm has a linear dependence on concentration in the numerator and an exponential function in the denominator. It can be described as follows:

$$q_e = \frac{K_R C_e}{1 + b_R C_e^m} \quad (4)$$

It has three isotherm constants, namely, K_R, b_R, and m.

3.5.4. Temkin Isotherm. The Temkin isotherm can be used to study the heat of adsorption and adsorbate−adsorbent interaction on the adsorbent surface.[41] Equation 5 shows the linear form of this isotherm:

$$q_e = B_1 \ln K_T + B_1 \ln C_e \quad (5)$$

where B_1 is the Temkin adsorption constant and K_T is the equilibrium binding constant (dm^3·mg^{-1}).

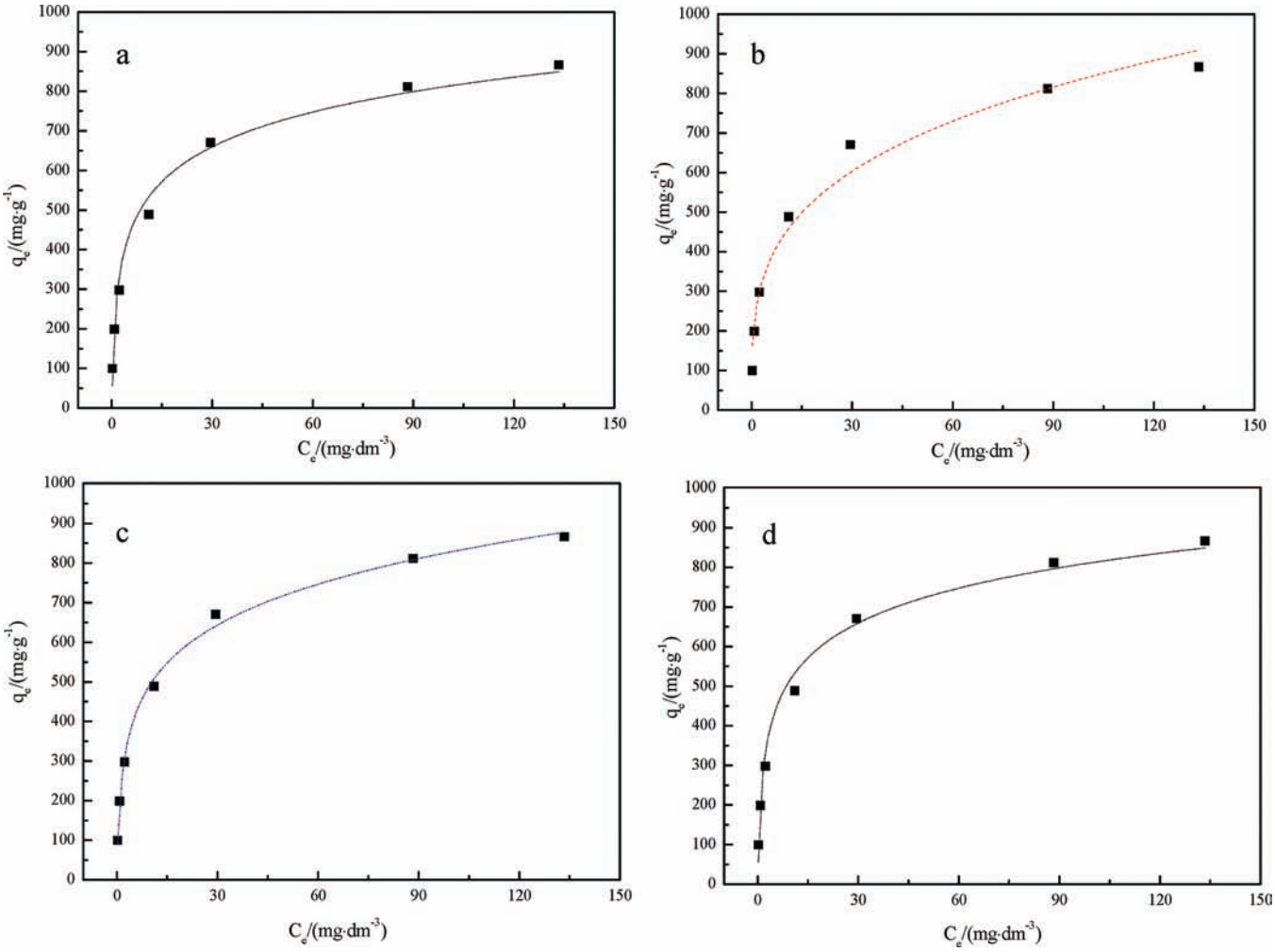

Figure 10. Isotherm models of (a) Langmuir, (b) Freundlich, (c) Redlich−Peterson, and (d) Temkin for adsorption of 2-NSA onto Fe-D301 (initial 2-NSA concentration, (100 to 1000) mg·dm^{-3}; contact time, 24 h; temperature, 298 K; agitation speed, 180 rpm).

Figure 9 shows the linear Temkin adsorption isotherm applied to the experimental data. Coefficients B_1 and K_T are easily obtained from the slope and intercept of the plot of q_e versus ln C_e. The Temkin adsorption isotherm indicated the heat of adsorption linearly increased as the thickness of the 2-NSA layer on the adsorbent gradually increased, because of reduced adsorbate−adsorbent interaction.[42] This model also assumes uniform distribution of binding sites on the surface of the adsorbent. The linear plot of this isotherm had a positive slope, which implies a repulsive lateral interaction exists in the adsorption layer.[43,44] The 2-NSA molecules initially occupy the active sites on the adsorbent surface. As 2-NSA coverage of the surface increases, the repulsive lateral interaction between the neighboring adsorbate molecules reduces the adsorption capacity.

The applicability of these isotherm equations was compared using the R^2 values. The adsorption isotherm results (Figure 10) indicate that the Redlich−Peterson and Temkin isotherms fit the data well (R^2 > 0.985) at all concentrations at 298 K. The constants of Langmuir, Freundlich, Redlich−Peterson, and Temkin isotherms at different temperatures were also evaluated (Table 2). The Redlich−Peterson model appeared to provide the best fit for the data at 298 K. The values of m were not close to unity, which indicates the isotherms are approaching the Freundlich but not the Langmuir model.

3.6. Thermodynamic Studies. To describe the thermodynamic behavior of adsorption of 2-NSA onto Fe-D301, the thermodynamic parameters free energy, ΔG^0, enthalpy change, ΔH^0, and entropy change, ΔS^0, were calculated for the adsorption process using the following equations:[45]

$$\Delta G^0 = \Delta H^0 - T\Delta S^0 \quad (6)$$

$$\ln\left(\frac{q_e}{C_e}\right) = \frac{\Delta S^0}{R} - \frac{\Delta H^0}{RT} \quad (7)$$

where q_e/C_e is the adsorption affinity and is a ratio of q_e to C_e. The values of ΔH^0 and ΔS^0 were determined from the slope and the intercept of the plots of $\ln(q_e/C_e)$ versus $1/T$ (Figure 11). The ΔG^0 values were calculated with eq 6. The thermodynamic parameters for the adsorption of 2-NSA onto Fe-D301 at various temperatures are summarized in Table 3. The negative ΔG^0 values at (298, 313, and 323) K indicate that the adsorption of 2-NSA onto Fe-D301 is favorable and spontaneous. ΔH^0 and ΔS^0 for the sorption process were calculated at −5.98 kJ·mol^{-1} and 11.42 J·(mol·K)$^{-1}$, respectively. The ΔH^0 was negative, which indicates that the adsorption reaction is exothermic. However, the adsorption capacity of 2-NSA increased with decreasing temperature. The positive ΔS^0 suggests increased

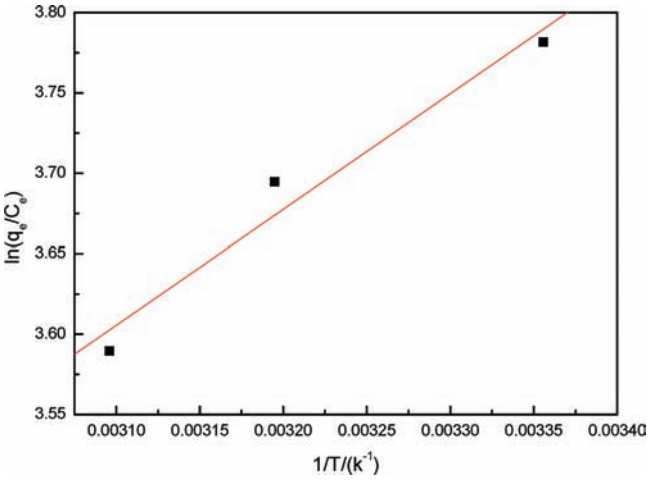

Figure 11. Thermodynamic study. ■, experiment data; red line, line fit.

Table 3. Values of Thermodynamic Parameters Evaluated for 2-NSA Sorption

	T	ΔG	ΔS	ΔH
adsorbent	K	kJ·mol^{-1}	J·(mol·K)$^{-1}$	kJ·mol^{-1}
Fe-D301	298	−9.39	11.42	−5.98
	313	−9.56		
	323	−9.67		

randomness at the solid−solution interface during the adsorption of 2-NSA onto Fe-D301.

3.7. Effect of Salts. Generally, wastewater contains more than one anion. Thus, the presence of other anions may interfere with the removal efficiency of 2-NSA. Common coexisting anions in wastewater with 2-NSA include SO_4^{2-} and SO_3^{2-}. Consequently, the selectivity of the adsorbent toward 2-NSA is of importance for field application. In this study, sodium sulfate (Na_2SO_4) and sodium sulfite (Na_2SO_3) were chosen as representative inorganic salts.[46] The effect of coexisting Na_2SO_4 and Na_2SO_3 on 2-NSA uptake by Fe-D301 resin was determined. The adsorption experiments were carried out in initial 2-NSA concentration range of (100 to 1000) mg·dm^{-3}. Figures 12, 13, and 14 show the effect of the Na_2SO_4, Na_2SO_3, and Na_2SO_4 and Na_2SO_3 on the 2-NSA removal efficiency and adsorption capacity. It was observed that the 2-NSA removal efficiency for Fe-D301 was higher than D301 significantly. When Na_2SO_4 coexisted, the 2-NSA adsorption capacity for Fe-D301 may increase 164.85 mg·g^{-1} compared with that of D301. 2-NSA removal efficiency was higher for low initial concentrations because of the availability of unoccupied binding sites on the adsorbents.

The SO_4^{2-} and SO_3^{2-} anions were able to adsorb onto the adsorbent. In general, the level of competitive adsorption varies from one anion to another and is related to a number of factors, such as molecular mass, ionic strength, and the number of π-bonds. The presence of SO_4^{2-} in the solution greatly reduced the adsorption capacity for 2-NSA, because it competed for available adsorption sites. Compared to SO_4^{2-}, the competitive adsorption of SO_3^{2-} was weak relatively. This difference in behavior may be attributed to the weaker dissociation of SO_3^{2-} compared to SO_4^{2-}.

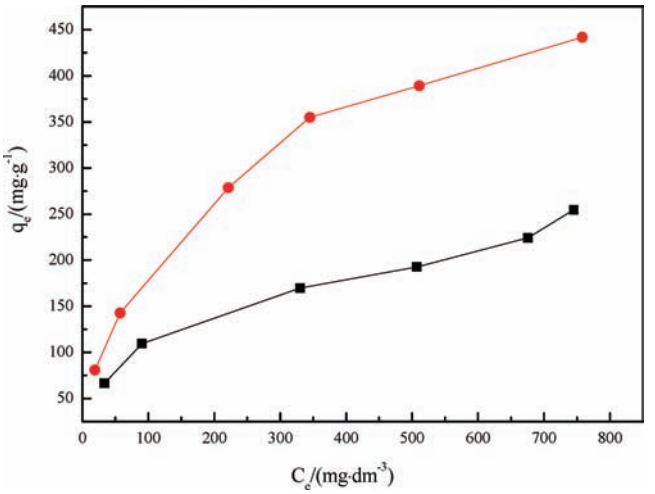

Figure 12. Effect of the added Na_2SO_4 on 2-NSA uptake onto D301 and Fe-D301 at 298 K (0.100 g of resin was introduced into 0.1 dm^3 of solution containing an initial 2-NSA amount of (100 to 1000) mg·dm^{-3} and 1 % Na_2SO_4). ■, D301; ●, Fe-D301.

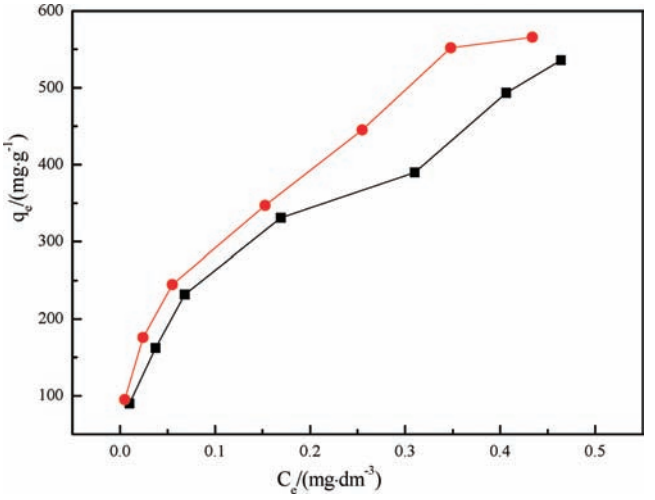

Figure 13. Effect of the added Na_2SO_3 on 2-NSA uptake onto D301 and Fe-D301 at 298 K (0.100 g of resin was introduced into 0.1 dm^3 of solution containing an initial 2-NSA amount of (100 to 1000) mg·dm^{-3} and 1 % Na_2SO_3). ■, D301; ●, Fe-D301.

3.8. Continuous Column-Mode Operation. Column studies are important because sewage is a continuously flowing system. Columns were designed to determine the breakthrough curve for the adsorption of 2-NSA from aqueous solution onto Fe-D301 resin. The effluent from the outlet of the column was analyzed for 2-NSA. The adsorption column was operated for 8 days, and a breakthrough curve was determined. The breakthrough curve (Figure 15) indicated that 2-NSA was efficiently removed by Fe-D301 within about 265 BV per run before substantial breakthrough occurred. The 2-NSA concentration in the effluent solution and its removal percentage for 307 BV was about 90.86 mg·dm^{-3} and 90.91 %, respectively. This adsorption capacity of Fe-D301 agreed with the adsorption capacity calculated using the batch adsorption technique.

dx.doi.org/10.1021/je2005984 |J. Chem. Eng. Data 2011, 56, 3881–3889

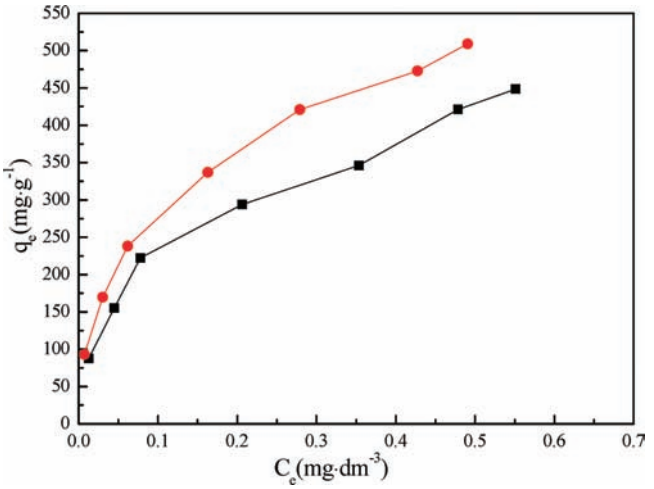

Figure 14. Effect of the added Na_2SO_4 and Na_2SO_3 on 2-NSA uptake onto D301 and Fe-D301 at 298 K (0.100 g of resin was introduced into 0.1 dm^3 of solution containing an initial 2-NSA amount of (100 to 1000) mg·dm^{-3}, 1 % Na_2SO_4, and 1 % Na_2SO_3). ■, D301; ●, Fe-D301.

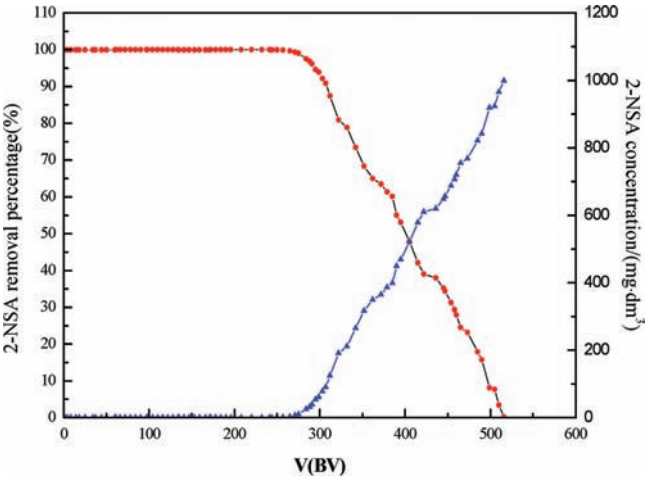

Figure 15. Column adsorption of 2-NSA onto Fe-D301 at 298 K. ●, removal percentage; ▲, concentration.

4. CONCLUSIONS

Iron impregnation of D301 resin provided a suitable adsorbent for the removal of 2-NSA from aqueous solution and sewage. The adsorption process was highly dependent on the pH of the solution, and at the optimum value, pH was 2.8. The removal percentage of 2-NSA using Fe-D301 resin was 85.60 % over 4 h. The removal rates increased with decreasing temperature but decreased with increasing initial concentration of 2-NSA. Equilibrium at the solid−solution interface was explained by the Redlich−Peterson adsorption isotherm. The thermodynamics of 2-NSA adsorption onto Fe-D301 resin confirmed the adsorption process was exothermic and spontaneous. A large increase in the adsorption capacity was observed for Fe-D301 comparing with D301 after addition of coexisting Na_2SO_4 and Na_2SO_3 to the 2-NSA solution. Results from preliminary column adsorption experiments were plotted as breakthrough curves and showed that the 2-NSA concentration and removal percentage in the effluent solution on 307 BV were about 90.86 mg·dm^{-3} and 90.91 %. Therefore, Fe-D301 resin is very effective for the removal of 2-NSA from aqueous solutions.

AUTHOR INFORMATION

Corresponding Author

*E-mail: changhaili@yahoo.cn.

Funding Sources

This research was funded by the Shandong Provincial Natural Science Foundation, China (Grant No. Z2008B06) and the Science Technology Development Program of Binzhou, China (Grant No. 200923).

REFERENCES

(1) Alonso, M. C.; Barcelo, D. Tracing polar benzene- and naphthalenesulfonates in untreated industrial effluents and water treatment works by ion-pair chromatography-fluorescence and electro spray-mass spectrometry. *Anal. Chim. Acta* **1999**, *400*, 211–231.

(2) Gonzalez-Martinez, S.; Pina-Mondragon, S.; Gonzalez-Barcelo, O. Treatment of the azo dye direct blue 2 in a biological aerated filter under anaerobic/aerobic conditions. *Water Sci. Technol.* **2010**, *61*, 789–796.

(3) Moghaddam, S. S.; Moghaddam, M. R. A.; Arami, M. Coagulation/flocculation process for dye removal using sludge from water treatment plant: Optimization through response surface methodology. *J. Hazard. Mater.* **2010**, *175*, 651–657.

(4) Sevimli, M. F.; Sarikaya, H. Z. Ozone treatment of textile effluents and dyes: effect of applied ozone dose, pH and dye concentration. *J. Chem. Technol. Biotechnol.* **2002**, *77*, 842–850.

(5) Kim, T. H.; Park, C.; Yang, J. M.; Kim, S. Comparison of disperse and reactive dye removals by chemical coagulation and Fenton oxidation. *J. Hazard. Mater.* **2004**, *112*, 95–103.

(6) Ghoreishi, S. M.; Haghighi, R. Chemical catalytic reaction and biological oxidation for treatment of non-biodegradable textile effluent. *Chem. Eng. J.* **2003**, *95*, 163–169.

(7) Chang, I. S.; Lee, S. S.; Choe, E. K. Digital textile printing (DTP) wastewater treatment using ozone and membrane filtration. *Desalination* **2009**, *235*, 110–121.

(8) Raghu, S.; Basha, C. A. Chemical or electrochemical techniques, followed by ion exchange, for recycle of textile dye wastewater. *J. Hazard. Mater.* **2007**, *149*, 324–330.

(9) Chen, Q. Q.; Wu, P. X.; Dang, Z.; Zhu, N. W.; Li, P.; Wu, J. H.; Wang, X. D. Iron pillared vermiculite as a heterogeneous photo-Fenton catalyst for photocatalytic degradation of azo dye reactive brilliant orange X−GN. *Sep. Purif. Technol.* **2010**, *71*, 315–323.

(10) Rezaee, A.; Ghaneian, M. T.; Taghavinia, N.; Aminian, M. K.; Hashemian, S. J. TiO_2 nanofibre assisted photocatalytic degradation of reactive blue 19 dye from aqueous solution. *Environ. Technol.* **2009**, *30*, 233–239.

(11) Suna, D.; Zhang, X. D.; Wu, Y. D.; Liu, X. Adsorption of anionic dyes from aqueous solution on fly ash. *J. Hazard. Mater.* **2010**, *181*, 335–342.

(12) Senthil Kumar, P.; Ramalingam, S.; Senthamarai, C.; Niranjanaa, M.; Vijayalakshmi, P.; Sivanesan, S. Adsorption of dye from aqueous solution by cashew nut shell: Studies on equilibrium isotherm, kinetics and thermodynamics of interactions. *Desalination* **2010**, *261*, 52–60.

(13) Hu, J. C.; Song, Z.; Chen, L. F.; Yang, H. J.; Li, J. L.; Richards, R. Adsorption properties of MgO (111) nanoplates for the dye pollutants from wastewater. *J. Chem. Eng. Data* **2010**, *55*, 3742–3748.

(14) Jain, N.; Basniwal, R. K.; Srivastava, A. K.; Jain, V. K. Reusable nanomaterial and plant biomass composites for the removal of methylene blue from water. *Environ. Technol.* **2010**, *31*, 755–760.

(15) Crini, G. Non-conventional low-cost adsorbents for dye removal: A review. *Bioresour. Technol.* **2006**, *97*, 1061–1085.

(16) Deo Mall, I.; Sivastava, V. C.; Agawal, N. K.; Misha, I. M. Adsorptive removal of malachite green dye from aqueous solution by

bagasse fly ash and activated carbon-kinetic study and equilibrium isotherm analyses. *Colloids Surf., A* **2005**, *264*, 17–28.

(17) Malana, M. A.; Ijaz, S.; Ashiq, M. N. Removal of various dyes from aqueous media onto polymeric gels by adsorption process: Their kinetics and thermodynamics. *Desalination* **2010**, *263*, 249–257.

(18) Jia, D. M.; Li, C. H.; Zhao, B. L.; Sun, S. Studies on the Adsorption of 2-Naphthalenesulfonic acid on basic resin from effluents. *J. Chem. Eng. Data* **2010**, *55*, 5801–5806.

(19) Anoop Krishnan, K.; Haridas, A. Removal of phosphate from aqueous solutions and sewage using natural and surface modified coir pith. *J. Hazard. Mater.* **2008**, *152*, 527–535.

(20) Namasivayam, C.; Sangeetha, D. Equilibrium and kinetic studies of adsorption of phosphate onto $ZnCl_2$ activated coir pith carbon. *J. Colloid Interface Sci.* **2004**, *280*, 359–365.

(21) Kasama, T.; Watanabe, Y.; Yamada, H.; Murakami, T. Sorption of phosphateson Al-pillared smectites and mica at acidic to neutral pH. *Appl. Clay Sci.* **2004**, *25*, 167–177.

(22) LeMire, L. E.; Teixeira, M. A.; Reed, B. E. Removal of As(V) using an iron-impregnated ion exchange bead. *Sep. Sci. Technol.* **2010**, *45*, 2051–2063.

(23) Chang, Q. G.; Lin, W.; Ying, W. C. Preparation of iron-impregnated granular activated carbon for arsenic removal from drinking water. *J. Hazard. Mater.* **2010**, *184*, 515–522.

(24) Reed, B.; Vaughan, R.; Jiang, L. Q. As(III), As(V), Hg, and Pb removal by Fe-oxide impregnated activated carbon. *J. Environ. Eng.* **2000**, *126*, 869–873.

(25) Payne, K.; Abdel-Fattah, T. Adsorption of arsenate and arsenite by iron-treated activated carbon and zeolites: effects of pH, temperature, and ionic strength. *J. Environ. Sci. Health, Part A* **2005**, *40*, 723–749.

(26) Chen, W. F.; Parette, R.; Zou, J.; Cannon, F. S. Arsenic removal by iron-modified activated carbon. *Water Res.* **2007**, *41*, 1851–1858.

(27) Hristovski, K. D.; Westerhoff, P. K.; Moller, T.; Sylverster, P. Effect of synthesis conditions on nano-iron (hydro)oxide impregnated granular activated carbon. *Chem. Eng. J.* **2009**, *146*, 237–243.

(28) Muniz, G.; Fierro, V.; Celzard, A.; Furdin, G.; Gonzalez-Sanchez, G.; Ballinas, M. L. Synthesis, characterization and performance in arsenic removal of iron-doped activated carbons prepared by impregnation with Fe(III) and Fe(II). *J. Hazard. Mater.* **2009**, *165*, 893–902.

(29) Azouaou, N.; Sadaoui, Z.; Djaafri, A.; Mokaddem, H. Adsorption of cadmium from aqueous solution onto untreated coffee grounds: Equilibrium, kinetics and thermodynamics. *J. Hazard. Mater.* **2010**, *184*, 126–134.

(30) Mishra, A.; Jha, B. Isolation and characterization of extracellular polymeric substances from micro-algae *Dunaliella salina* under salt stress. *Bioresour. Technol.* **2009**, *100*, 3382–3386.

(31) Gong, C.; Chen, D.; Jiao, X.; Wang, Q. Continuous hollow α-Fe_2O_3 and α-Fe fibers prepared by the sol−gel method. *J. Mater. Chem.* **2002**, *12*, 1844–1847.

(32) Keiser, J. T.; Brown, C. W.; Heidersbach, R. H. The electrochemical reduction of rust films on weathering surface. *J. Electrochem. Soc.* **1982**, *129*, 2686–2689.

(33) Roonasi, P.; Holmgren, A. An ATR−FTIR study of sulphate sorption on magnetite; rate of adsorption, surface speciation, and effect of calcium ions. *J. Colloid Interface Sci.* **2009**, *333*, 27–32.

(34) Johnson, S. B.; Franks, G. V.; Scales, P. J.; Boger, D. V.; Healy, T. W. Surface chemistry−rheology relationships in concentrated mineral suspensions. *Int. J. Miner. Process* **2000**, *58*, 267–304.

(35) Dutta, P. K.; Ray, A. K.; Sharma, V. K.; Millero, F. J. Adsorption of arsenate and arsenite on titanium dioxide suspensions. *J. Colloid Interface Sci.* **2004**, *278*, 270–275.

(36) Nassar, N. N. Rapid removal and recovery of Pb(II) from wastewater by magnetic nanoadsorbents. *J. Hazard. Mater.* **2010**, *184*, 538–546.

(37) Moussavi, G.; Khosravi, R. Removal of cyanide from wastewater by adsorption onto pistachio hull wastes: Parametric experiments, kinetics and equilibrium analysis. *J. Hazard. Mater.* **2010**, *183*, 724–730.

(38) Langmuir, I. The constitution and fundamental properties of solids and liquids. Part I. Solids. *J. Am. Chem. Soc.* **1916**, *38*, 2221–2295.

(39) Freundlich, H. M. F. Uber die adsorption in losungen. *Z. Phys. Chem.* **1906**, *57*, 385–470.

(40) Redlich, O.; Peterson, D. L. A useful adsorption isotherm. *J. Phys. Chem.* **1959**, *63*, 1024.

(41) Gad, H. M. H.; El-Sayed, A. A. Activated carbon from agricultural by-products for the removal of Rhodamine-B from aqueous solution. *J. Hazard. Mater.* **2009**, *168*, 1070–1081.

(42) Sharma, Y. C.; Uma; Upadhyay, S. N. Removal of a cationic dye from wastewaters by adsorption on activated carbon developed from coconut coir. *Energy Fuels* **2009**, *23*, 2983–2988.

(43) De Souza, F.; Spinelli, A. Caffeic acid as a green corrosion inhibitor for mild steel. *Corros. Sci.* **2009**, *51*, 642–649.

(44) Khaled, K. Monte Carlo simulations of corrosion inhibition of mild steel in 0.5 M sulphuric acid by some green corrosion inhibitors. *J. Solid State Electrochem.* **2009**, *13*, 1743–1756.

(45) Barsanescu, A.; Buhaceanu, R.; Dulman, V. Removal of basic blue 3 by sorption onto a weak acid acrylic resin. *J. Appl. Polym. Sci.* **2009**, *113*, 607–614.

(46) Pan, B. C.; Zhang, Q. X.; Meng, F. W.; Li, X. T.; Zhang, X.; Zheng, J. Z.; Zhang, W. M.; Pan, B. J.; Chen, J. L. Sorption enhancement of aromatic sulfonates onto an aminated hyper-cross-linked polymer. *Environ. Sci. Technol.* **2005**, *39*, 3308–3313.